Cancer Letters 357 (2015) 393–403

Contents lists available at ScienceDirect

Cancer Letters

journal homepage: www.elsevier.com/locate/canlet

Original Articles

# Alantolactone selectively suppresses STAT3 activation and exhibits potent anticancer activity in MDA-MB-231 cells

Jaemoo Chun [a], Rui-Juan Li [b], Mao-Sheng Cheng [b], Yeong Shik Kim [a,*]

[a] Natural Products Research Institute, College of Pharmacy, Seoul National University, Seoul 151-742, Republic of Korea
[b] Key Laboratory of Structure-Based Drugs Design & Discovery, Ministry of Education, School of Pharmaceutical Engineering, Shenyang Pharmaceutical University, Shenyang 110-016, China

ARTICLE INFO

*Article history:*
Received 17 September 2014
Received in revised form 21 November 2014
Accepted 24 November 2014

*Keywords:*
STAT3
Alantolactone
Sesquiterpene lactone
MDA-MB-231 cells
Triple-negative breast cancer (TNBC)

ABSTRACT

The important goal of cancer drug discovery is to develop therapeutic agents that are effective, safe, and affordable. In the present study, we demonstrated that alantolactone, which is a sesquiterpene lactone, has potential activity against triple-negative breast cancer MDA-MB-231 cells by suppressing the signal transducer and activator of transcription 3 (STAT3) signaling pathway. Alantolactone effectively suppressed both constitutive and inducible STAT3 activation at tyrosine 705. Alantolactone decreased STAT3 translocation to the nucleus, its DNA-binding, and STAT3 target gene expression. Alantolactone significantly inhibits STAT3 activation with a marginal effect on MAPKs and on NF-κB transcription; however, this effect is not mediated by inhibiting STAT3 upstream kinases. Although SHP-1, SHP-2, and PTEN, which are protein tyrosine phosphatases (PTPs), were not affected by alantolactone, the treatment with a PTP inhibitor reversed the alantolactone-induced suppression of STAT3 activation, indicating that PTP plays an important role in the action of alantolactone. Finally, alantolactone treatment resulted in the inhibition of migration, invasion, adhesion, and colony formation. The *in vivo* administration of alantolactone inhibited the growth of human breast xenograft tumors. These results provide preclinical evidence to continue the development of alantolactone as a STAT3 inhibitor and as a potential therapeutic agent against breast cancer.



## Introduction

Signal transducer and activator of transcription 3 (STAT3) is an oncogenic transcription factor associated with the proliferation, metastasis, angiogenesis, and chemo-resistance of cancer cells [1,2]. Under normal conditions, STAT3 activation is tightly regulated by the presence or absence of polypeptide ligands bound to its receptor. However, in cancer cells, cytokine and growth factor receptors become constitutively activated, most commonly by autocrine or paracrine expression of their respective ligands, similar to interleukin 6 (IL-6), epidermal growth factor (EGF), and platelet-derived growth factor (PDGF) [3]. Consequently, activated STAT3 has been found in numerous solid tumors, including breast, prostate, pancreas, and ovarian cancers. Recent studies have shown that STAT3 is constitutively activated in approximately 70% of breast cancers [4] but is most associated with triple-negative breast cancer (TNBC), which lacks estrogen receptors, progesterone receptors, and HER2 expression [5]. In breast cancer cells, active STAT3 was found in TNBC cells alone. Surprisingly, 80% of TNBC cells express activated STAT3 [6]. TNBC cells additionally produce a high amount of IL-6, which allows STAT3 activation to respond to IL-6 stimulation in an autocrine manner [7]. Abnormal activation of STAT3, which is prevalent in TNBC, plays a critical role in invasion and metastasis [8]. TNBC is generally characterized by an aggressive clinical course, with poor prognosis [9]. However, no proven targeted therapy is currently available for TNBC. Therefore, targeting STAT3 in TNBC could be an important therapeutic approach in the treatment of TNBC.

STAT3 is an important point of convergence for several signaling pathways in cancer cells. Activated STAT3 forms dimers through reciprocal phosphotyrosine-SH2 interactions between STAT3 monomers. In turn, STAT3 dimers translocate to the nucleus and activate target gene transcription. STAT3 upregulates the expression of genes that regulate protection against apoptosis, such as Bcl-2 and Bcl-xL; the cell cycle, such as cyclin $D_1$ and c-myc; proliferation, such as COX-2; angiogenesis, such as VEGF; metastasis, such as CXCR4; and invasion, such as MMP-9 [10]. Because these gene products are closely related to tumor development, regulating the STAT3 signaling pathway is critical to cell proliferation, invasion, angiogenesis, and tumor immune evasion [11]. STAT3 is well established as a crucial biological abnormality involved in the molecular processes leading to cancer development [12]. Therefore, many efforts are under way to discover small molecules that are able to directly inhibit STAT3 activation. Although several small molecules reportedly inhibit STAT3 signaling, most of these molecules

* Corresponding author. Tel.: +82 2 880 2479; fax: +82 2 765 4768.
*E-mail address:* kims@snu.ac.kr (Y.S. Kim).

http://dx.doi.org/10.1016/j.canlet.2014.11.049
0304-3835/

indirectly suppress STAT3 activation and act on targets other than STAT3 [13]. Additionally, numerous small molecules with biochemical targets block STAT3 signaling by inhibiting STAT3 upstream kinases [12]. Therefore, finding a novel small molecule that can selectively inhibit STAT3 activation is required.

Alantolactone, a major constituent of *Inula helenium*, has recently been reported to possess various pharmacological activities, such as anti-inflammation [14] and apoptosis induction [15]; however, the exact mechanism of this anticancer activity remains unclear. In the present study, we investigated the inhibitory effect of alantolactone on STAT3 activation, its molecular mechanism, and its applications in TNBC MDA-MB-231 cells, which could play an important role in the prevention and treatment of cancer.

## Materials and methods

### *Chemicals and reagents*

Alantolactone (purity >98%) was purchased from Tauto Biotech (Shanghai, China). Alantolactone was dissolved in DMSO and the final concentration of DMSO in the cell culture was kept below 0.05%. Dulbecco's phosphate buffered saline (DPBS), a protease inhibitor cocktail, 3-(4,5-dimethylthiazol-2-yl)-2,5-diphenyltetrazolium bromide (MTT), SP600125, S3I-201, and doxorubicin were purchased from Sigma Aldrich (St. Louis, MO). EGF and IL-6 were purchased from R&D Systems (Minneapolis, MN). Matrigel was purchased from BD Biosciences (San Jose, CA). The primary antibodies for p-STAT3 (Tyr705), p-STAT3 (Ser727), STAT3, p-JAK1, p-JAK2, and CXCR4 were from Abcam (Cambridge, MA). The primary antibodies for PARP1, p-JNK, JNK, p-ERK, ERK, COX-2, SHP-1, SHP-2, PTEN, p65, p50, c-Rel, p-STAT1, STAT1, p-STAT5, STAT5, p-STAT6, STAT6, and β-actin and all secondary antibodies were from Santa Cruz Biotechnology (Santa Cruz, CA). The primary antibodies for p-Akt, Akt, p-EGFR, EGFR, cyclin $D_1$, c-Jun, p-FAK, and FAK were from Epitomics (Burlingame, CA). The primary antibodies for p-Src, Src, c-Myc, c-Fos, p-c-Jun, JAK1, and JAK2 were from Cell Signaling Technology (Beverly, MA). The primary antibody for Ki-67 was from Dako (Glostrup, Denmark). Penicillin, streptomycin, DMEM (high glucose), RPMI 1640 medium and fetal bovine serum (FBS) were obtained from GenDepot (Barker, TX).

### *Cell culture*

MDA-MB-231 and MCF-7 human breast cancer cells were obtained from the Korea Cell Bank (Seoul, Korea). MCF-10A human breast normal cells were obtained from the American Type Culture Collection (Rockville, MD). MDA-MB-231 and MCF-7 cells were maintained in DMEM supplemented with 10% FBS and antibiotics (penicillin 100 U/mL and streptomycin 100 μg/mL). MCF-10A cells were maintained in DMEM supplemented with 10% FBS, 20 ng/mL EGF, 500 ng/mL hydrocortisone (Sigma Aldrich), and antibiotics. Cultures were maintained in an incubator at 37 °C in 5% $CO_2$.

### *Preparation of whole cell lysates and nuclear extracts*

Whole cell lysates were prepared using a lysis buffer (20 mM HEPES, pH 7.6, 350 mM NaCl, 20% glycerol, 0.5 mM EDTA, 0.1 mM EGTA, 1% NP-40, 50 mM NaF, 0.1 mM DTT, 0.1 mM PMSF, and protease inhibitor cocktail) for 30 min on ice. The lysates were centrifuged at 15,000 rpm for 10 min. Nuclear extracts were prepared using a lysis buffer (10 mM HEPES, pH 7.9, 10 mM KCl, 0.1 mM EDTA, 0.1 mM EGTA, 1 mM DTT, 1 mM PMSF, and protease inhibitor cocktail) for 15 min on ice. Then, 10% NP-40 was added and the mixtures were centrifuged for 5 min. The nuclear pellets were resuspended in nuclear extraction buffer (20 mM HEPES, pH 7.9, 400 mM NaCl, 1 mM EDTA, 1 mM EGTA, 1 mM DTT, 1 mM PMSF, and protease inhibitor cocktail) and centrifuged at 15,000 rpm for 10 min. The protein concentration was determined by the Bradford reagent (Bio-Rad, Hercules, CA).

### *Western blotting*

Equal amounts of protein were separated on 8–12% SDS-PAGE and semi-dry transferred to nitrocellulose membranes. The membranes were blocked with 5% skim milk, incubated with the respective antibodies overnight at 4 °C, and incubated with HRP-conjugated secondary antibody for 2 h. Finally, the immunoreactive bands were developed using a chemiluminescence kit (Intron Biotechnology, Seoul, Korea). Densitometric measurements of the bands from Western blotting were performed using the digitalized scientific software program UN-SCAN-IT (Silk Scientific Corporation, Orem, UT). The values above the figures represent the relative density of the bands normalized to β-actin or PARP1.

### *Electophoretic mobility shift assay (EMSA)*

To determine the STAT3, AP-1, or NF-κB DNA-binding activity, EMSA was performed as previously described [16]. Briefly, the nuclear extracts were incubated with a $^{32}$P-end-labeled double-stranded STAT3 consensus oligonucleotide (Santa Cruz Biotechnology) with the sequence 5′-GATCCTTCTGGGATTTCCTAGATC-3′, AP-1 consensus oligonucleotide (Promega, Madison, WI) with the sequence 5′-CGCTTGATGAGTCAG CCGGAA-3′ or NF-κB consensus oligonucleotide (Promega) with the sequence 5′-AGTTGAGGGGACTTTCCCAGGC-3′. For the competition assay, 100-fold excess of unlabeled oligonucleotide was added to the binding reaction for 10 min before adding the labeled probe. After binding, the DNA–protein complexes were subjected to 6% PAGE. The radioactive bands were analyzed using BAS-1500 image analyzer (Fujifilm, Tokyo, Japan).

### *Molecular docking*

Our structure-based virtual screening employed molecular docking program Sybyl (version 6.5) and Autodock (version 4.0). Schematic representation was generated by Discovery Studio (version 3.0). The X-ray crystal structure of the STAT3 homodimer bound to DNA solved at 2.25-Å resolution was retrieved from Protein Data Bank (PDB code: 1BG1) for docking simulation. Double-stranded DNA, all crystallographic water, and $PO_4^{3-}$ buffer molecules were removed. STAT3 monomer was added pol-Hydrogen, given Kullman-Uni charge, and minimized by Sybyl. The native pTyr peptide was extracted from the crystal structure of one of the monomers as a ligand. The centroid of ligand is used as center of the gridbox, whose number grid points in XYZ is $20 \times 20 \times 20$, and spacing is 0.375-Å. The box could cover the entire region of STAT3 SH2 domain–pTyr interaction. The residues within the gridbox were used to construct the grids for docking small-molecule alantolactone with STAT3 SH2 domain.

### *Wound-healing assay*

To determine cell motility, the cells were seeded into 12-well plates and grown to 80–90% confluence. A monolayer of cells was scratched with a sterile micropipette tip, followed by washing with DPBS to remove cellular debris. The cells were exposed to alantolactone, and cell migration was observed and counted under a CKX41 microscope (Olympus, Tokyo, Japan) at a magnification of 100×. The cells that migrated across the black lines were counted in five randomly chosen fields from each triplicate treatment. The percentage of inhibition was expressed using untreated wells at 100%.

### *Cell invasion assay*

Cell invasion assay was conducted using Transwell chambers (SPL, Seoul, Korea). Transwell inserts with 8 μm pore size were coated with matrigel (1 mg/mL) and dried for 30 min. The cells treated with alantolactone were suspended in serum-free DMEM. Approximately $5 \times 10^4$ cells per insert were added to the upper chambers, and DMEM was added to the lower chambers. After incubating for 24 h, the non-invasive cells that remained on the upper side of the insert were removed using cotton swabs. The cells that invaded on the lower side of the insert were stained with 2% crystal violet and observed under a CKX41 microscope at a magnification of 200×. To quantify the invasiveness of the cells, methanol was added to dissolve the stain and the absorbance was determined at a wavelength of 595 nm.

### *Cell-matrix adhesion assay*

Cell adhesion assay was carried out using the CytoSelect™ cell adhesion assay (Cell Biolabs, San Diego, CA). The cells treated with alantolactone were suspended in DMEM and added to each well coated with fibronectin, collagen type I, collagen type IV, laminin, fibrinogen, or BSA. The plate was then incubated at 37 °C in 5% $CO_2$ for 90 min. The cells were stained with stain solution, and the stained cells were dissolved in extraction solution. The results were obtained by measuring the absorbance at a wavelength of 595 nm using a microplate reader (Molecular Devices, Sunnyvale, CA).

### *Cell viability assay*

Cell viability was evaluated using MTT assay. The cells were seeded into 96-well plates and maintained at 37 °C for 24 h. The cells were treated with alantolactone for 24 h. The MTT solution (0.5 mg/mL) was added to each well, and the cells were incubated for another 3 h. The MTT formazan crystals were dissolved in DMSO. The results were obtained by measuring the absorbance at a wavelength of 540 nm using a microplate reader.

### *Gelatin zymography*

Gelatin zymography was performed to determine the activity of MMP-9 in culture medium as previously described [17]. Briefly, the cells were seeded into 12-well plates and replaced with serum-free DMEM. The cells were then exposed to alantolactone for 24 h, and the supernatants were subjected to 8% SDS-PAGE gels containing 0.1% gelatin. The gels were washed with 2.5% Triton X-100 and incubated in developing buffer (50 mM Tris–Cl, pH 7.6, 200 mM NaCl, 10 mM $CaCl_2$) at 37 °C for 24 h. The gelatinolytic activity of MMP-9 was visualized by staining the gels with 0.1% Coomassie blue R-250 in 45% methanol/10% acetic acid for 30 min and destaining with 45% methanol/10% acetic acid.

*Clonogenic assay*

To determine long-term effects, the cells were cultured at 500 cells/well in a 24-well plate with DMEM. The cells were then exposed to alantolactone for 24 h. After being rinsed with fresh DMEM, cells were allowed to grow for 10 days until the colonies were visible. Then, cells were fixed, stained with 2% crystal violet in ethanol, and photographed.

*Cell cycle analysis*

Cell cycle phase distribution was assessed using a FACSCalibur flow cytometer (BD Biosciences). After treatment with alantolactone, MDA-MB-231 cells were collected by trypsinization and washed with DPBS. The cells were fixed with 70% ethanol and incubated at −20 °C overnight. The cells were then collected by centrifugation. The pellet was washed, suspended in DPBS, and incubated with RNase A (50 μg/mL) at room temperature for 30 min. The cells were stained with PI (50 μg/mL) for 10 min, and the DNA content was measured using flow cytometry and analyzed using the CellQuest software (BD Biosciences).

*Tumor xenograft study and immunohistochemistry*

Animal care and experimental procedures were conducted in accordance with the guidelines of Seoul National University Institutional Animal Care and Use Committees (approval ID: 130417-5). Female athymic BALB/c nude mice at the age of 6 weeks were purchased from the NaraBiotech (Seoul, Korea). MDA-MB-231 cells ($5 \times 10^6$ cells/200 μL) were subcutaneously injected into the right flanks of the mice. Ten days after the injection of cells, mice were randomly divided into treatment and control groups ($n = 5$). The animals were administered alantolactone (2.5 mg/kg of body weight, suspended in DMSO 0.1% v/v, 100 μL i.p. injection) every 2 days, whereas control animals were treated with an equal volume of saline (DMSO 0.1% v/v, 100 μL i.p. injection). Tumor volume was measured using a caliper according to the following formula: $\text{length} \times \text{width}^2 \times \pi/6$. After 14 days of treatment, the mice were sacrificed and the tumors were removed, weighed, and fixed in 4% paraformaldehyde for immunohistochemical analysis. Tumor tissues were embedded in paraffin, and the paraffin sections were incubated with antibodies against Ki-67 and p-STAT3 (1:200 dilution). The sections were developed using the HPR EnVision™ System (Dako), and the peroxidase binding sites were detected by staining with 3,3′-diaminobenzidinetetrahydrochloride (Dako). Finally, sections were counterstained with Mayer's hematoxylin and mounted. The stained sections were observed under a microscope.

*Statistical analysis*

All the data are presented as the mean ± SD from at least three independent experiments. An analysis of variance (ANOVA) with the Dunnett's *t*-test was used for the statistical analysis of multiple comparisons. A value of $p < 0.05$ was chosen as the criterion for statistical significance.

## Results

### *Alantolactone suppresses constitutive STAT3 tyrosine phosphorylation*

To clarify the molecular mechanisms by which alantolactone inhibits STAT3 activation, first, we evaluated its effect on STAT3 phosphorylation at tyrosine 705 in MDA-MB-231 cells. Alantolactone significantly inhibited STAT3 phosphorylation at all time points studied, although alantolactone had a less inhibitory effect after 24 h (Fig. 1A). These results suggest that the suppression of STAT3 phosphorylation by alantolactone lasted for 12 h with a maximum inhibition. Moreover, at the initial time point, alantolactone inhibited STAT3 phosphorylation at tyrosine 705 in a dose- and time-dependent manner; however, this treatment did not affect STAT3 phosphorylation at serine 727. The total STAT3 protein levels were not affected by alantolactone (Fig. 1B). Because STAT3 phosphorylation at tyrosine 705 leads to STAT3 dimerization and then nuclear translocation, we determined whether alantolactone suppresses the nuclear translocation of STAT3. Consistent with the inhibition of STAT3 phosphorylation, alantolactone inhibited STAT3 translocation to the nucleus (Fig. 1C). Next, we confirmed that alantolactone suppresses the DNA-binding activity of STAT3 (Fig. 1D). In addition, we investigated whether the alantolactone-induced inhibition of STAT3 phosphorylation is reversible. The results demonstrated that alantolactone suppressed STAT3 phosphorylation and that removing alantolactone gradually increased STAT3 phosphorylation without changing total STAT3 expression (Fig. 1E). Next, we used several breast cell lines, MDA-MB-231, MCF-10A, and MCF-7. The results demonstrated that alantolactone significantly inhibited STAT3 phosphorylation in MDA-MB-231 cells highly expressing active STAT3 (Fig. 1F). To investigate whether alantolactone selectively inhibits STAT3 phosphorylation, we examined the effect of alantolactone on the activation of other STATs, including STAT1, STAT3, STAT5, and STAT6. We found that alantolactone did not inhibit the phosphorylation of STAT1 and slightly inhibited STAT5 and STAT6 phosphorylation. However, alantolactone treatment almost completely inhibited STAT3 phosphorylation (Fig. 1G), suggesting that alantolactone selectively inhibits STAT3 activation.

### *Alantolactone inhibits IL-6- or EGF-induced STAT3 phosphorylation*

IL-6-stimulated STAT3 phosphorylation is an accepted model for studying STAT3 inhibition [18]. Hence, we examined whether alantolactone inhibits IL-6-stimulated STAT3 phosphorylation. As shown in Fig. 2A, IL-6 (10 ng/mL) treatment resulted in STAT3 activation. However, pretreatment with alantolactone significantly inhibited IL-6-induced STAT3 activation. In addition, this pretreatment decreased STAT3 activation to levels below that in unstimulated cells. EGF activates STAT3 via gp130-independent EGFR [19]. We examined whether alantolactone inhibits EGF-stimulated STAT3 phosphorylation. As shown in Fig. 2B, EGF (100 ng/mL) treatment resulted in EGFR and STAT3 activation. However, pretreatment with alantolactone significantly inhibited EGF-induced STAT3 activation. Alantolactone treatment did not affect EGFR and Akt phosphorylation. We also confirmed that alantolactone inhibited IL-6-induced STAT3 phosphorylation for 30 min and EGF-induced STAT3 phosphorylation for 10 min in a dose-dependent manner (Fig. 2C).

### *Tyrosine phosphatase inhibitor abrogates alantolactone-induced inhibition of STAT3 phosphorylation*

Tyrosine residues on STAT proteins are phosphorylated by various upstream signaling cascades, including JAKs, Src, PI3K/Akt, and MAPKs [20]. To determine whether the inhibitory effect of alantolactone on STAT3 phosphorylation is due to the suppression of upstream signaling pathways, we evaluated the effect of alantolactone on the activation of JAK1, JAK2, and Src in MDA-MB-231 cells. Alantolactone did not reduce the protein levels of phosphorylated JAK1, JAK2, and Src (Fig. 2D). In contrast, JAK1 and Src phosphorylation was slightly elevated by alantolactone. The total protein levels of JAK1, JAK2, and Src were not altered by alantolactone, suggesting that alantolactone inhibits STAT3 phosphorylation independent of the upstream kinases JAK1, JAK2, and Src. Because protein tyrosine phosphatases (PTPs) have been reported to negatively regulate STAT3 activation [13], we assessed the potential role of upstream PTPs in the alantolactone-induced inhibition of STAT3 phosphorylation. The PTPs implicated in regulating STAT3 signaling include SHP-1, SHP-2, and PTEN [21]. However, the protein expression levels of these three tyrosine phosphatases were not affected by alantolactone (Fig. 2E). Conversely, treatment with pervanadate, which is a broad-acting tyrosine phosphatase inhibitor, prevented the alantolactone-induced suppression of STAT3 activation (Fig. 2F). These results suggest that PTP activation plays an important role in suppressing STAT3 phosphorylation by alantolactone. In addition, alantolactone decreased the phosphorylation of FAK, EGFR, Akt, and ERK (Fig. 2G). These results also indicate that STAT3 inhibition occurs as early as 30 min, when the phosphorylation of these proteins is scarcely affected. This finding suggests that the decreased p-FAK, EGFR, Akt, and ERK levels at 4 h could be events secondary to STAT3 inhibition and that the effects of alantolactone are highly selective for the STAT3 pathway over the FAK, EGFR, Akt, and ERK signaling pathways.

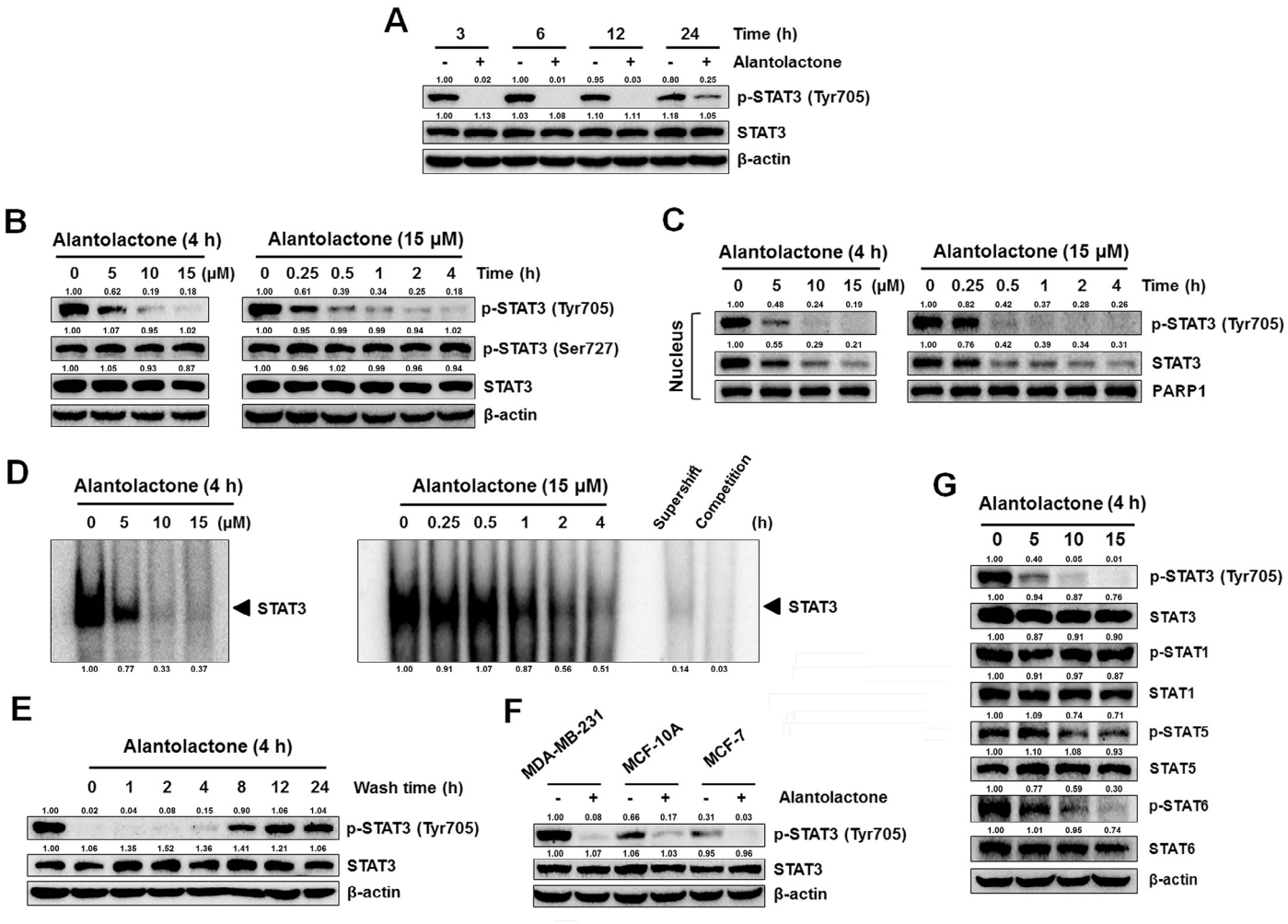


**Fig. 1.** Inhibitory effect of alantolactone on STAT3 activation. (A) Effect of alantolactone on constitutively active STAT3 phosphorylation at Tyr705. The cells were treated with alantolactone for 3, 6, 12, and 24 h. (B) Effect of alantolactone on STAT3 phosphorylation at Tyr705 and Ser727. The cells were treated with the indicated concentrations of alantolactone for the indicated times. The cell lysates were subjected to Western blotting to determine the p-STAT3 (Tyr705 and Ser727) and STAT3 protein levels. (C) Effect of alantolactone on STAT3 nuclear translocation. Nuclear extracts were subjected to Western blotting to determine STAT3 nuclear translocation. (D) Effect of alantolactone on the DNA-binding activity of STAT3. Nuclear extracts were incubated with a $^{32}$P-labeled STAT3 consensus oligonucleotide and subjected to 6% PAGE. (E) Effect of alantolactone on the reversibility of STAT3 inhibition. The cells were treated with alantolactone for 4 h, washed with DPBS to remove alantolactone, and then resuspended in fresh medium for the indicated times. The whole cell lysates were analyzed using Western blotting. (F) Effect of alantolactone on STAT3 activation in MDA-MB-231, MCF-10A, and MCF-7 cells. (G) Effect of alantolactone on the activation of STAT1, STAT5, and STAT6. The cells were treated with alantolactone for 4 h. The cell lysates were subjected to Western blotting for p-STATs and STATs.

### *Alantolactone is predicted to bind to STAT3 SH2 domain by computational docking*

We performed a structure-based molecular docking study explaining the significant interactions between alantolactone and STAT3. The structural composition and topological analyses of the STAT3 SH2 domain binding "hotspot" indicated three subpockets on the STAT3 protein surface, including the key pTyr705-binding region. The upper subpocket was composed of the residues Phe716, Met660, Ile659, Tyr657, and Trp623. The left subpocket was composed of the residues Arg609, Ser611, Glu612, Ser613, Val619, Thr620, Thr622, Val637, Glu638, and Pro639. The right subpocket was composed of the residues Lys 591, Glu594, Arg595, Ile634, Gln635, and Ser636. The three solvent-accessible subpockets of the SH2 domain surface were accessed by alantolactone. These results indicated that alantolactone was predicted to project into the right subpocket (Fig. 3A). Within the binding pocket, Arg595 was predicted to form hydrogen bonds with alantolactone (Fig. 3B).

### *Alantolactone sensitizes doxorubicin chemotherapy in STAT3-overexpressing MDA-MB-231 cells*

Aberrant STAT3 expression has been shown to confer drug resistance. Recent studies have shown that doxorubicin-resistant MDA-MB-231 cells show an abnormal increase in STAT3 activity and that higher STAT3 activation correlates with drug resistant profiles of recurrent tumors [22]. As shown in Fig. 3C, doxorubicin exposure for 72 h notably increased STAT3 phosphorylation in MDA-MB-231 cells, indicating that doxorubicin treatment further enhances STAT3 activation. However, alantolactone significantly reduced STAT3 phosphorylation, suggesting that suppressing STAT3 activation may overcome doxorubicin resistance. In addition, alantolactone enhanced the antiproliferative effect of doxorubicin at 72 h (Fig. 3D). These results suggest that the suppression of STAT3 activation by alantolactone is a possible strategy to increase tumor cell response to cytotoxic agents.

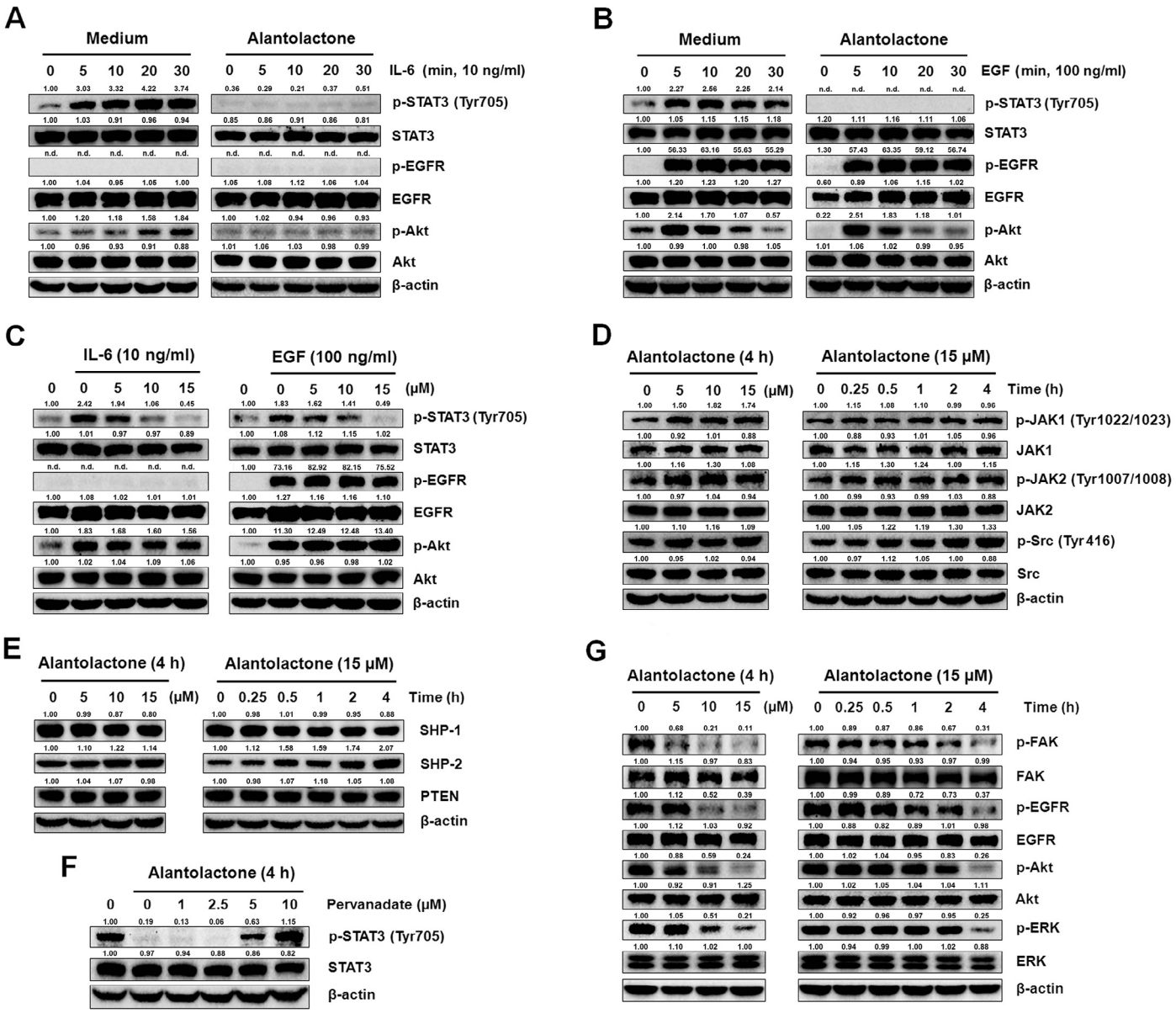


**Fig. 2.** Effect of alantolactone on inducible STAT3 activation and STAT3 upstream signaling pathways in MDA-MB-231 cells. (A) The cells were pretreated with alantolactone for 4 h and stimulated with IL-6 (10 ng/mL) for the indicated times. (B) The cells were pretreated with alantolactone for 4 h and stimulated with EGF (100 ng/mL) for the indicated times. (C) The cells were pretreated with the indicated concentration of alantolactone for 4 h and stimulated with IL-6 for 30 min and with EGF for 10 min. Whole cell lysates were subjected to Western blotting to determine the p-STAT3 (Tyr705), STAT3, p-EGFR, EGFR, p-ERK, ERK, p-Akt, and Akt protein levels. (D) Effect of alantolactone on the JAKs and Src signaling pathways. The cells were treated with the indicated concentrations of alantolactone for the indicated times. Cell lysates were subjected to Western blotting with antibodies against p-JAK1, JAK1, p-JAK2, JAK2, p-Src, and Src. (E) Effect of alantolactone on three specific tyrosine phosphatases, including SHP-1, SHP-2, and PTEN. The cell lysates were subjected to Western blotting with antibodies against SHP-1, SHP-2, and PTEN. (F) Effect of alantolactone on PTPs. First, the cells were treated with the indicated concentration of pervanadate for 30 min, followed by 15 μM alantolactone for 4 h, and the cell lysates were subjected to Western blotting to determine the p-STAT3 (Tyr705) and STAT3 protein levels. (G) Effect of alantolactone on the FAK, EGFR, Akt, and ERK pathways. Cell lysates were subjected to Western blotting with antibodies against p-FAK, FAK, p-EGFR, EGFR, p-mTOR, mTOR, p-Akt, Akt, p-ERK, and ERK.

*Alantolactone activates the JNK/AP-1 signaling pathway*

To understand the possible upstream signaling pathways in alantolactone-treated MDA-MB-231 cells, we evaluated JNK phosphorylation using Western blotting. Alantolactone increased JNK phosphorylation at an early time point, when alantolactone-induced STAT3 inhibition occurs (Fig. 4A). We investigated whether alantolactone increases the protein level on c-Jun and c-Fos, which are components of the AP-1 complex, which is a downstream target of the JNK pathway. As shown in Fig. 4B, alantolactone increased c-Jun and p-c-Jun expression, but had no effect on c-Fos expression. As shown in Fig. 4C, the DNA-binding activity of AP-1 was increased by alantolactone. These results suggest that the JNK activation by alantolactone led to increased AP-1 transcriptional activity. To further determine whether the JNK/AP-1 activation by alantolactone was associated with the inhibition of STAT3 activation, the cells were pretreated with the JNK inhibitor SP600125. The results demonstrated that SP600125 suppressed alantolactone-induced JNK phosphorylation. However, the SP600125-induced inhibition of JNK phosphorylation did not block the alantolactone-induced inhibition of STAT3 phosphorylation (Fig. 4D). We additionally used S3I-201, a commercially available STAT3 inhibitor, which selectively inhibited STAT3 activity and induced growth inhibition in cells

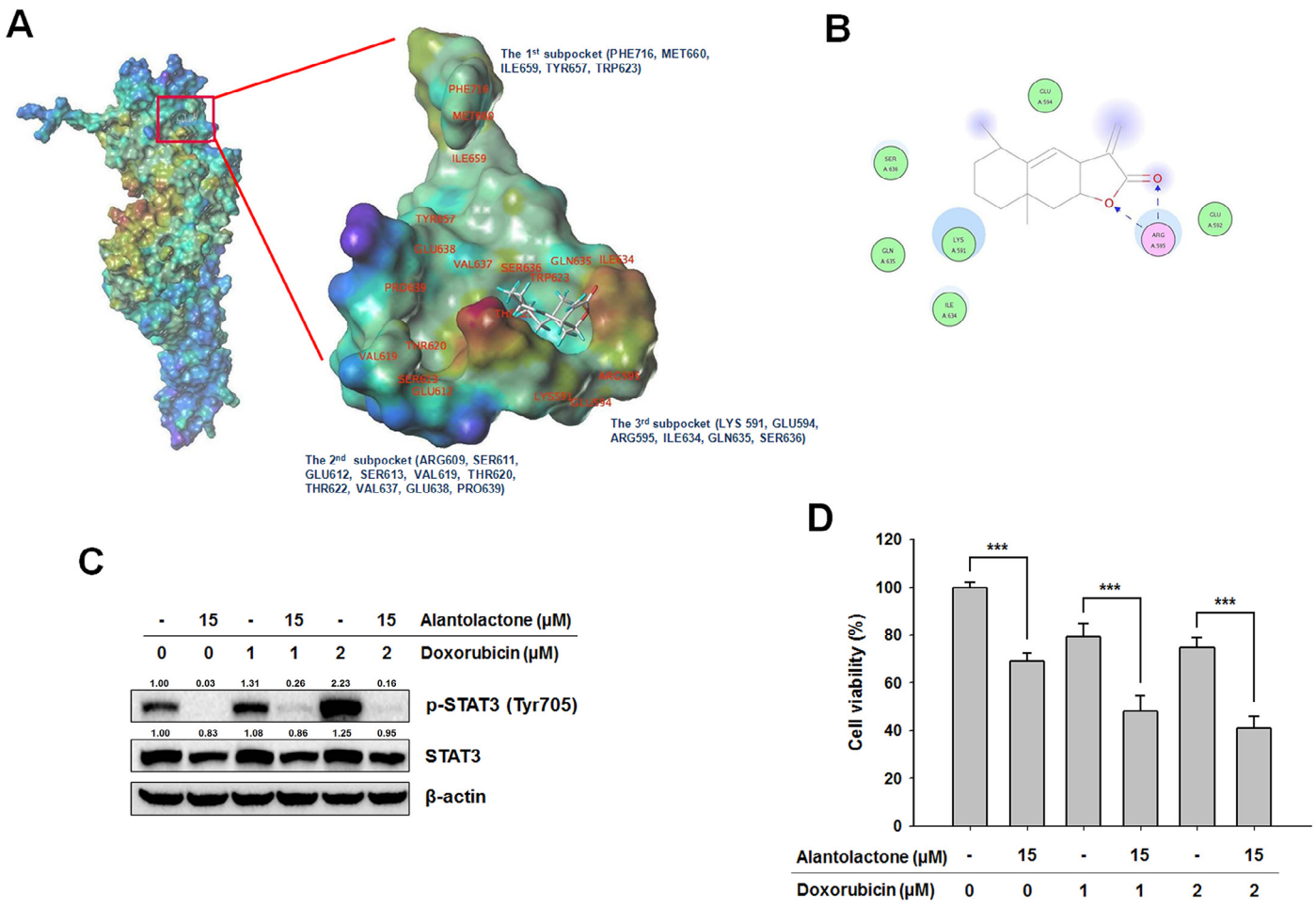


**Fig. 3.** Computational modeling of alantolactone binding to the STAT3 SH2 domain and the combined effect of alantolactone and doxorubicin on STAT3 activation. (A) Schematic representation of interactions between the STAT3 SH2 domain and alantolactone, generated using the Discovery Studio software. (B) H-bonding interactions are indicated as blue arrows. (C) Combinational effect of alantolactone and doxorubicin on STAT3 activation. The cells were pretreated with 1 and 2 μM of doxorubicin for 72 h and exposed to alantolactone for 4 h. The cell lysates were subjected to Western blotting to determine the p-STAT3 (Tyr705) and STAT3 protein levels. (D) Combined effect of alantolactone and doxorubicin on MDA-MB-231 cell proliferation. The cells were pretreated with 1 and 2 μM of doxorubicin for 72 h and exposed to alantolactone for an additional 24 h. Cell viability was determined using the MTT assay. Significant difference compared with the vehicle-treated control, $^{***}p < 0.001$. (For interpretation of the references to color in this figure legend, the reader is referred to the web version of this article.)

with persistent pSTAT3 expression [23]. We compared the inhibitory effect of alantolactone and S3I-201 on STAT3 activation to evaluate the potency of alantolactone as a STAT3 inhibitor. As shown in Fig. 4E, S3I-201 selectively inhibited STAT3 phosphorylation but increased JNK phosphorylation in a dose-dependent manner. Importantly, alantolactone had a greater inhibitory effect on STAT3 tyrosine phosphorylation and on cyclin $D_1$ protein expression than S3I-201, despite the low alantolactone concentration used. However, alantolactone did not affect STAT3 serine phosphorylation, whereas S3I-201 inhibited STAT3 serine phosphorylation. Altogether, these results suggest that alantolactone selectively inhibits STAT3 tyrosine phosphorylation and activates the JNK pathway independent of STAT3 inhibition.

*Alantolactone inhibits NF-κB translocation to the nucleus*

STAT3 is known to interact with NF-κB in various cancer models. STAT3 and NF-κB have been shown to cooperate in promoting cell growth by interacting at different levels of their activating pathways [24]. Therefore, we confirmed the changes in the nuclear translocation and DNA-binding activity of NF-κB. As shown in Fig. 4F, alantolactone suppressed NF-κB DNA-binding activity. Our results also demonstrated that alantolactone inhibited the translocation of NF-κB subunits, including c-Rel, p65, and p50 (Fig. 4G). These results suggest that STAT3 inhibition could decrease NF-κB translocation to the nucleus.

*Alantolactone inhibits the migration, invasion, adhesion, growth, and colony formation of MDA-MB-231 cells harboring constitutively active STAT3*

The data presented thus far demonstrate that alantolactone effectively blocks STAT3 activation and suppresses several signaling pathways associated with malignant transformation. Therefore, we investigated whether alantolactone suppresses the migration, invasion, and adhesion of MDA-MB-231 cells. Alantolactone treatment for 24 h significantly decreased cell motility (Fig. 5A) and cell invasion (Fig. 5B) in a dose-dependent manner. Alantolactone treatment for 24 h markedly reduced the number of cells attached to ECM molecules (Fig. 5C). Furthermore, the inhibitory effect of alantolactone on the reproductive ability of cells was determined using a colony formation assay with MDA-MB-231 cells. As shown in Fig. 5D, alantolactone substantially suppressed colony formation, suggesting that the effect of alantolactone on cancer cells was irreversible. In addition, we compared the inhibitory effects of

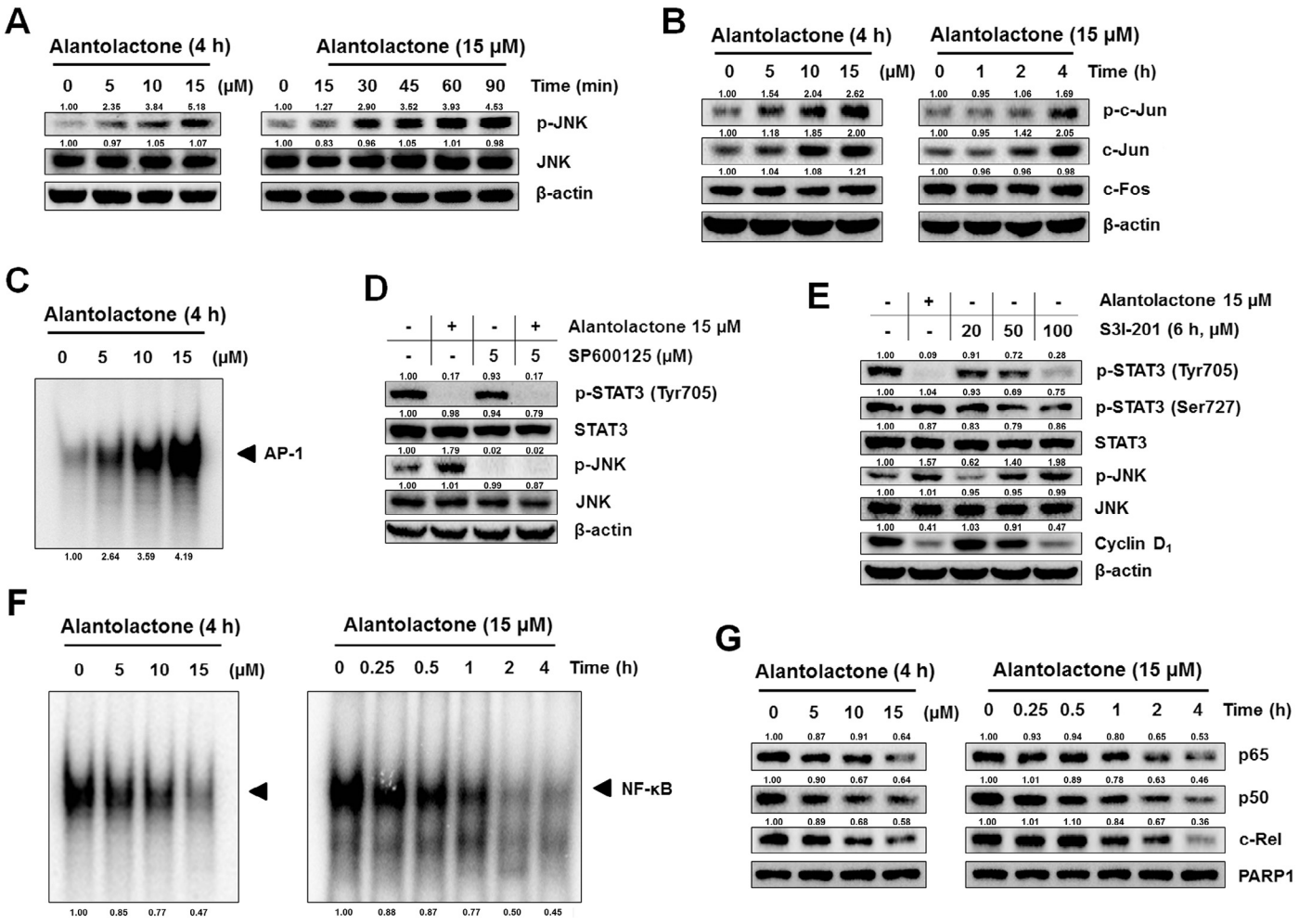


**Fig. 4.** Effect of alantolactone on JNK phosphorylation and NF-κB activation in MDA-MB-231 cells. (A) Dose and time-course study of the effect of alantolactone on JNK phosphorylation. The cell lysates were subjected to Western blotting with antibodies against p-JNK and JNK. (B) Effect of alantolactone on c-Jun phosphorylation and the total levels of c-Jun and c-Fos protein expression. The cell lysates were subjected to Western blotting with antibodies against p-c-Jun, c-Jun, and c-Fos. (C) Effect of alantolactone on the DNA-binding activity of AP-1. Nuclear extracts were incubated with a $^{32}$P-labeled AP-1 consensus oligonucleotide and subjected to 6% PAGE. (D) Effect of the JNK inhibitor (SP600125) on alantolactone-mediated STAT3 inhibition. SP600125 was applied for 4 h before alantolactone treatment for 4 h. The cell lysates were subjected to Western blotting with antibodies against p-STAT3, STAT3, p-JNK, and JNK. (E) Effect of the STAT3 inhibitor S3I-201 and the potency of alantolactone as a STAT3 inhibitor. The cells were treated with alantolactone or with S3I-201 for 6 h. Whole cell lysates were subjected to Western blotting for p-STAT3 (Tyr705), p-STAT3 (Ser727), STAT3, p-JNK, JNK, and cyclin $D_1$. (F) Effect of alantolactone on the DNA-binding activity of NF-κB. Nuclear extracts were incubated with a $^{32}$P-labeled NF-κB consensus oligonucleotide and subjected to 6% PAGE. (G) Effect of alantolactone on nuclear translocation. Nuclear extracts were subjected to Western blotting to determine the nuclear translocation of NF-κB subunits, including c-Rel, p65, and p50.

alantolactone on cell growth in MDA-MB-231, MCF-10A, and MCF-7 cells. As shown in Fig. 5E, alantolactone significantly inhibited cell proliferation in MDA-MB-231 cells compared with MCF-10A and MCF-7 cells. MMP-9 is a STAT3 target gene that contributes to migration and invasion [25]. Alantolactone markedly inhibited the gelatinolytic activity of MMP-9 (Fig. 5F). Next, we assessed the effect of alantolactone on STAT3 target genes products. The results demonstrated that the expression levels of STAT3 target genes that regulate proliferation (cyclin $D_1$, c-myc, and COX-2) and metastasis (CXCR4) were decreased by alantolactone (Fig. 5G). These results suggest that inhibiting aberrantly active STAT3 suppresses STAT3-dependent gene regulation. In addition, alantolactone induced a depletion of cells in the $G_1$ phase and a concomitant accumulation of cells in the $G_2$/M phase (Appendix: Supplementary Fig. S1). We also evaluated whether alantolactone could indirectly affect STAT3 upstream proteins, such as JAKs, Src, and ERK, at later time points. As shown in Fig. 5H, alantolactone treatment for 24 h decreased the phosphorylation of STAT3 (Tyr705), JAK1, JAK2, Src, and ERK without affecting their total protein levels. These results suggest that alantolactone selectively inhibits STAT3 phosphorylation, thereby inhibiting the secondary signaling events to STAT3 inhibition and suppressing cell proliferation. Additionally, this inhibition might be associated with IL-6 inhibition by repressing STAT3 transcriptional activity.

### *Alantolactone inhibits the tumor growth of MDA-MB-231 xenografts in nude mice*

To confirm the antitumor effect of alantolactone *in vivo*, we performed a xenograft assay of MDA-MB-231 cells. Athymic nude mice were subcutaneously injected with the cells and i.p. administered 2.5 mg/kg of alantolactone for 14 days. We found that the average tumor volume in the alantolactone-treated mice was approximately 2.17-fold lower compared with that in the control mice (Fig. 6A). However, the administration of alantolactone did not affect the overall body weight during the experimental period, suggesting no apparent toxicity (Fig. 6B).

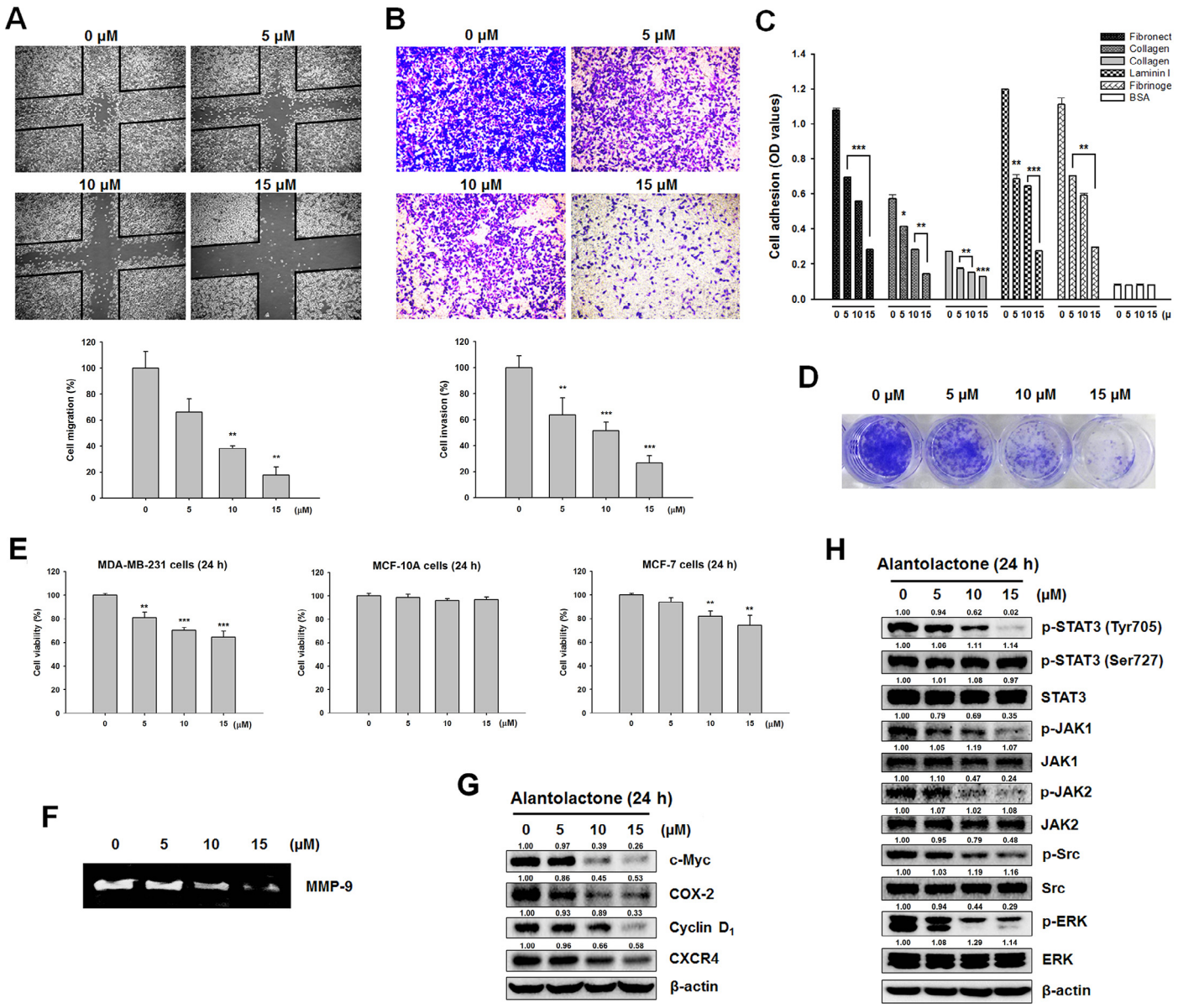


**Fig. 5.** Effect of alantolactone on MDA-MB-231 cell migration, invasiveness, ECM molecule adhesion, and colony formation. (A) For the migration assay, cell monolayers were scratched with a micropipette tip, and the cells were exposed to alantolactone for 24 h. The cells were observed under a microscope at 100× magnification. (B) For the invasion assay, the cells treated with alantolactone for 24 h were seeded onto Matrigel-coated Transwell chambers and incubated for 24 h. The invading cells were stained with crystal violet and observed under a microscope at 200× magnification. (C) For the adhesion assay, the cells treated with alantolactone for 24 h were added to the indicated ECM-coated plate. The adherent cells were stained with stain solution, and the absorbance was measured at 595 nm. Significant difference compared with vehicle-treated control, $^{*}p < 0.01$, $^{**}p < 0.01$, and $^{***}p < 0.001$. (D) The cells were incubated with alantolactone for 24 h, changed with fresh medium, and allowed to grow into colonies for 10 days. The cells were fixed, stained with crystal violet, and photographed. (E) The anti-proliferative effect of alantolactone on MDA-MB-231, MCF-10A, and MCF-7 cells. The cells were treated with alantolactone for 24 h. Cell viability was determined using MTT assay. Significant difference compared with the vehicle-treated control, $^{**}p < 0.01$ and $^{***}p < 0.001$. (F) Effect of alantolactone on the proteolytic activity of MMP-9. The cells were exposed to alantolactone for 24 h. The conditioned media were subjected to gelatin zymography to analyze the proteolytic activity of MMP-9. (G) Effect of alantolactone on STAT3-regulated gene products. The cells were treated with alantolactone for 24 h. Whole cell lysates were subjected to Western blotting for c-Myc, COX-2, cyclin $D_1$, and CXCR4. (H) Effect of alantolactone on STAT3-associated protein expression levels. The cell lysates were subjected to Western blotting for p-STAT3, STAT3, p-JAK1, JAK1, p-JAK2, JAK2, p-Src, Src, p-ERK, and ERK.

Additionally, the average tumor weight was significantly lower in the alantolactone-treated mice compared with the control mice (Fig. 6C). We additionally determined whether the alantolactone-mediated suppression of tumor growth was accompanied by the inhibition of STAT3 activation and cell proliferation. The administration of alantolactone resulted in a significant decrease in p-STAT3 and cyclin $D_1$ expression in the tumor tissues (Fig. 6D), consistent with the results from the *in vitro* assay. Immunohistochemical studies demonstrated that the levels of STAT3 and Ki-67 protein expression were lower in the alantolactone-treated mice compared with those in the control mice (Fig. 6E). These results fully support our *in vitro* results described above, suggesting that alantolactone suppresses tumor growth by inhibiting STAT3 activation in the MDA-MB-231 xenograft tumors.

## Discussion

STAT3 activation has been associated with the survival, proliferation, metastasis, and chemo-resistance of cancer cells. Thus, STAT3

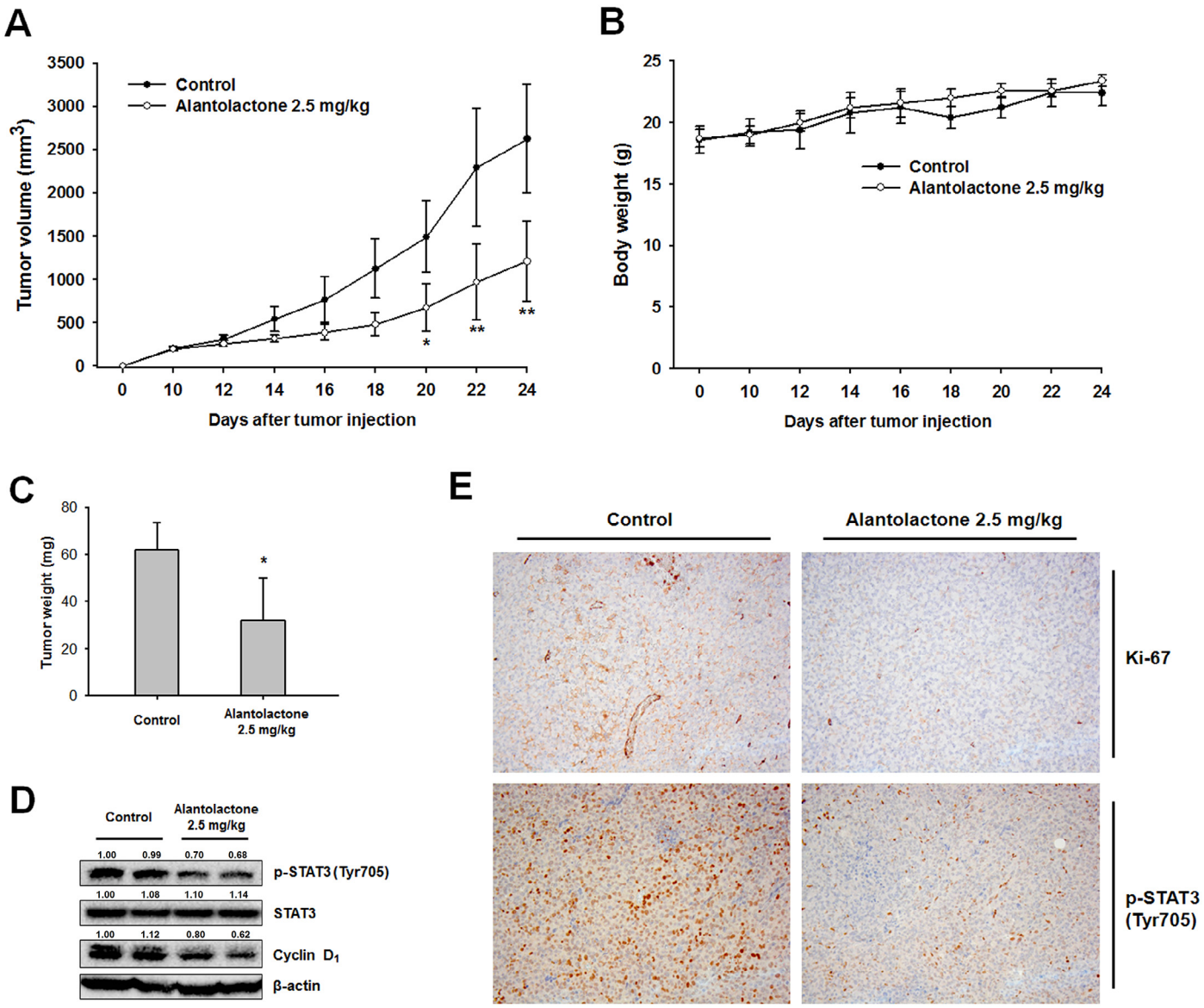


**Fig. 6.** Effect of alantolactone on tumor growth in xenografted nude mice. (A) BALB/c nude mice were subcutaneously injected with MDA-MB-231 cells and intraperitoneally administered 2.5 mg/kg of alantolactone or vehicle control for 14 days (every 2 days). Tumor volumes were measured with a caliper every 2nd day. Significant difference compared with the control group, $^{*}p < 0.05$ and $^{**}p < 0.01$. (B) The body weight changes were monitored during the test period. (C) The average weight of the tumors from mice. (D) Protein expressions in tumor tissues. The levels of p-STAT3 and cyclin $D_1$ proteins in the tumor sections were assessed using Western blotting. (E) Expression of Ki-67 and p-STAT3 (brown) in the tumor tissues, as determined by immunohistochemistry. Tumor tissues from representative animals were embedded in paraffin, and the paraffin sections were incubated with the antibodies for Ki-67 and p-STAT3. (For interpretation of the references to color in this figure legend, the reader is referred to the web version of this article.)

inhibitors have potential uses in the treatment and prevention of cancer [26]. In the present study, we identified alantolactone, which is a sesquiterpene lactone primarily isolated from *I. helenium*, as a novel STAT3 inhibitor. We demonstrated for the first time that alantolactone can suppress STAT3 activation in the TNBC cell line MDA-MB-231. By selectively inhibiting STAT3 phosphorylation at Tyr705, alantolactone suppressed STAT3 nuclear translocation and DNA-binding activities. Alantolactone also suppressed IL-6- or EGF-induced STAT3 activation in MDA-MB-231 cells.

The mechanism by which alantolactone inhibits STAT3 activation was investigated in detail in the present study. STAT3 activation is negatively regulated through numerous mechanisms, including suppressor of cytokine signaling (SOCS) proteins and various PTPs [27]. SOCS proteins directly inhibit JAKs by binding to the receptor or to the JAK activation loop [28]. The activation of JAKs and Src has been closely associated with STAT3 activation [23]. However, alantolactone did not affect the levels of phosphorylated JAK1, JAK2, and Src proteins. These results suggest that alantolactone selectively inhibits STAT3 phosphorylation regardless of the upstream kinases JAKs and Src in MDA-MB-231 cells. PTPs, such as SHP-1, SHP-2, and PTEN, negatively regulate STAT3 activation. PTPs can directly dephosphorylate the receptor tyrosine kinases, JAKs or STAT3, thus ensuring STAT3 signaling termination [13]. However, PTP inhibition by pervanadate reversed the alantolactone-induced inhibition of STAT3 phosphorylation, although the levels of PTPs were not affected by alantolactone. Thus, we suggest that PTP also plays an important role in the action of alantolactone. Many studies suggest that PTP activity is negatively regulated by the SH2 domains and the binding to SH2 domain stimulates the phosphatase activity [29]; however, further studies are required to understand the detailed

mechanism of the STAT3-dephosphorylating PTPs activated by alantolactone. Among other STAT family members (STAT1, STAT3, STAT5, and STAT6), alantolactone notably inhibited STAT3 expression. The STAT3 protein regulates several aspects of growth, survival and differentiation in cells by regulating the transcription of STAT3 target genes. The fact that alantolactone inhibits expression of c-myc, COX-2, cyclin $D_1$, and CXCR4 suggests that alantolactone acts as an anticancer agent. STAT3 forms a homodimer or heterodimer with STAT1 to activate the transcription of target genes. However, STAT3 homodimerization is the predominant form of activated STAT3 in breast cancer cells [30]. Using computational modeling, we found that alantolactone possibly directly binds to the SH2 domain of STAT3. These findings further strengthen our hypothesis that alantolactone selectively inhibits STAT3 activation. Recently, several studies have suggested that the suppression of STAT3 activation can be a potential target for chemosensitizing strategies because the constitutive activation of STAT3 signaling confers cell resistance to apoptosis in various cancer cells [31]. Our results confirmed that STAT3 plays a role in the cell resistance to doxorubicin exhibited by the TNBC cell line MDA-MB-231. Surprisingly, alantolactone reduced the doxorubicin-induced STAT3 phosphorylation and exhibited a chemosensitizing effect. These results suggest that alantolactone, as an inhibitor of STAT3, may overcome resistance to chemotherapy in TNBC.

Crosstalk between STAT3 and NF-κB has been demonstrated at multiple levels, including STAT3 activation and cancer cell invasion. STAT3 can trap constitutively activated NF-κB within the nucleus of cancer cells [32]. Maintaining NF-κB activity in tumors requires STAT3, which is constitutively activated as well [33]. In addition, both STAT3 and NF-κB activation induces changes in the expression of multiple target genes associated with survival, proliferation, and apoptosis, including Bcl-2, cyclin $D_1$, and c-myc [34]. Recent reports indicated that the inhibition of STAT3 phosphorylation may synergistically affect the transcriptional activity of NF-κB [35]. In the present study, alantolactone activated the JNK/AP-1 pathway independent of STAT3 inhibition. In addition, alantolactone inhibited STAT3 phosphorylation after a shorter incubation and at concentrations lower than those required for NF-κB inhibition, suggesting that alantolactone directly suppressed STAT3 phosphorylation and was independent of NF-κB inhibition. Nevertheless, higher alantolactone concentrations decreased NF-κB nuclear translocation and its DNA-binding activity, consistent with the inhibition of STAT3 nuclear translocation and its DNA-binding activity. Altogether, alantolactone potentially inhibits the STAT3 and NF-κB interconnecting signaling pathways.

We designed the current study to further evaluate the action of alantolactone, particularly with respect to the STAT3 signaling pathway. We performed our study by performing a functional assay, which measures the motility, invasiveness, and adhesion of cancer cells *in vitro*. We demonstrated that alantolactone inhibited the migration, invasion, and adhesion of MDA-MB-231 cells. Interestingly, alantolactone treatment remarkably inhibited the growth of MDA-MB-231 cells, which express constitutively activated STAT3, but had little or no effect on the proliferation of MCF-10A and MCF-7 cells, which do not express activated STAT3. In addition, alantolactone was shown to inhibit colony formation. Several small molecule STAT3 inhibitors reduced the migration and invasion of these cancer cells, and the effects of these inhibitors are known to cross-talk with NF-κB signaling [26]. Our results are consistent with these reports demonstrating that the inhibition of STAT3 signaling results in the inhibition of migration, invasion, and adhesion. However, alantolactone did not induce apoptosis in the range of 5–15 μM (data not shown). These results suggest that the suppression of STAT3 phosphorylation by alantolactone is not correlated with the

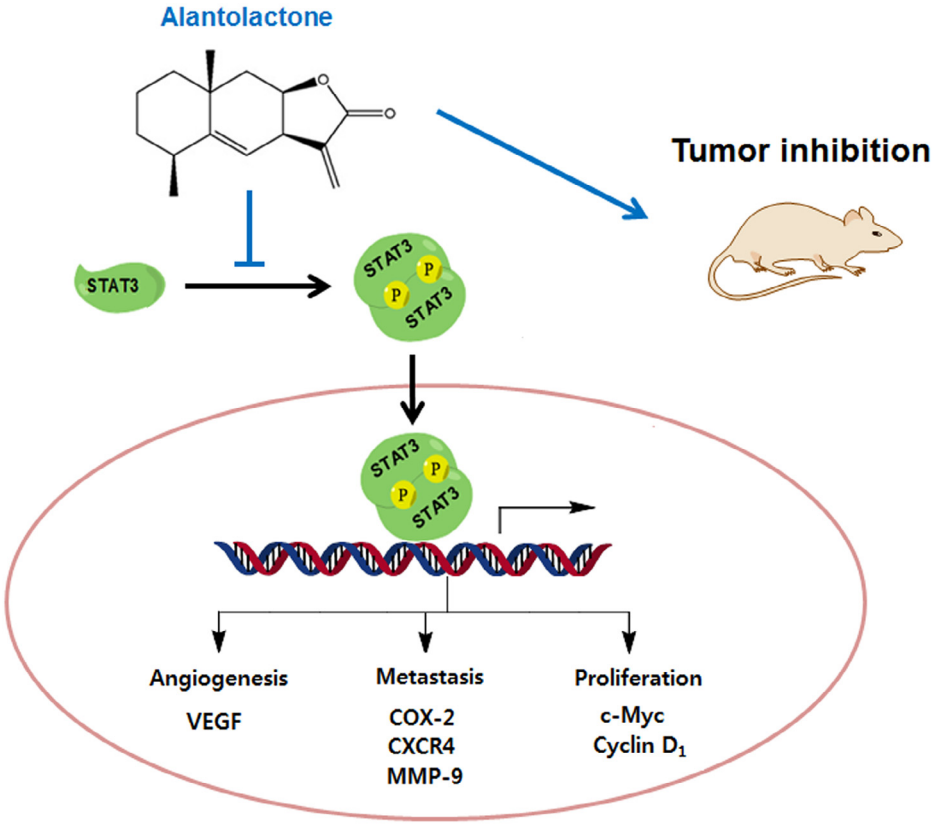


**Fig. 7.** A schematic model of alantolactone's activity in the STAT3 signaling pathway.

induction of apoptosis. Finally, we demonstrated that alantolactone inhibits tumor growth in a human breast xenograft model. We observed an *in vivo* inhibitory action of alantolactone consistent with lowered p-STAT3 and cyclin $D_1$ levels in tumor tissues, suggesting that the inhibition of STAT3 signaling by alantolactone is an important mechanism for the *in vivo* efficacy of alantolactone.

In conclusion, alantolactone completely suppressed inducible and constitutively activated STAT3 and blocked the nuclear translocation and the DNA-binding activity of STAT3 in MDA-MB-231 cells (Fig. 7). Alantolactone treatment additionally resulted in the inhibition of migration, invasion, adhesion, and colony formation. Alantolactone (2.5 mg/kg) administration significantly suppressed the growth of human breast cancer cell xenograft tumors. These results provide the preclinical evidence for further development of alantolactone as a STAT3 inhibitor and as a potential agent against TNBC.

## Acknowledgment

This work was supported by an MRC grant from the National Research Foundation of Korea (No. 2009-93146).

## Conflict of interest

The authors have no conflict of interest to declare.

## Appendix: Supplementary material

Supplementary data to this article can be found online at doi:10.1016/j.canlet.2014.11.049.

## References

[1] K. Abubaker, R.B. Luwor, R. Escalona, O. McNally, M.A. Quinn, E.W. Thompson, et al., Targeted disruption of the JAK2/STAT3 pathway in combination with systemic administration of paclitaxel inhibits the priming of ovarian cancer stem cells leading to a reduced tumor burden, Front. Oncol. 4 (2014) 75.
[2] G. Vitale, S. Zappavigna, M. Marra, A. Dicitore, S. Meschini, M. Condello, et al., The PPAR-γ agonist troglitazone antagonizes survival pathways induced by STAT-3 in recombinant interferon-β treated pancreatic cancer cells, Biotechnol. Adv. 30 (2012) 169–184.
[3] H. Yu, R. Jove, The STATs of cancer – new molecular targets come of age, Nat. Rev. Cancer 4 (2004) 97–105.
[4] S.R. Kim, H.S. Seo, H.S. Choi, S.G. Cho, Y.K. Kim, E.H. Hong, et al., *Trichosanthes kirilowii* ethanol extract and cucurbitacin D inhibit cell growth and induce apoptosis through inhibition of STAT3 activity in breast cancer cells, Evid. Based Complement. Alternat. Med. 2013 (2013) 975350.
[5] S.R. Walker, M. Xiang, D.A. Frank, Distinct roles of STAT3 and STAT5 in the pathogenesis and targeted therapy of breast cancer, Mol. Cell. Endocrinol. 382 (2014) 616–621.
[6] L.L. Marotta, V. Almendro, A. Marusyk, M. Shipitsin, J. Schemme, S.R. Walker, et al., The JAK2/STAT3 signaling pathway is required for growth of CD44+ CD24– stem cell-like breast cancer cells in human tumors, J. Clin. Invest. 121 (2011) 2723–2735.
[7] T. Ara, Y.A. Declerck, Interleukin-6 in bone metastasis and cancer progression, Eur. J. Cancer 46 (2010) 1223–1231.
[8] H.J. Lee, N.J. Seo, S.J. Jeong, Y. Park, D.B. Jung, W. Koh, et al., Oral administration of penta-*O*-galloyl-β-D-glucose suppresses triple-negative breast cancer xenograft growth and metastasis in strong association with JAK1-STAT3 inhibition, Carcinogenesis 32 (2011) 804–811.
[9] M. De Laurentiis, D. Cianniello, R. Caputo, B. Stanzione, G. Arpino, S. Cinieri, et al., Treatment of triple negative breast cancer (TNBC): current options and future perspectives, Cancer Treat. Rev. 36 (2010) S80–S86.
[10] I. Podolak, A. Galanty, D. Sobolewska, Saponins as cytotoxic agents: a review, Phytochem. Rev. 9 (2010) 425–474.
[11] C. Rivat, S. Rodrigues, E. Bruyneel, G. Pietu, A. Robert, G. Redeuilh, et al., Implication of STAT3 signaling in human colonic cancer cells during intestinal trefoil factor 3 (TFF3) – and vascular endothelial growth factor-mediated cellular invasion and tumor growth, Cancer Res. 65 (2005) 195–202.
[12] M. Zhao, B. Jiang, F.H. Gao, Small molecule inhibitors of STAT3 for cancer therapy, Curr. Med. Chem. 18 (2011) 4012–4018.
[13] Z.Y. Yu, R. Huang, H. Xiao, W.F. Sun, Y.J. Shan, B. Wang, et al., Fluacrypyrim, a novel STAT3 activation inhibitor, induces cell cycle arrest and apoptosis in cancer cells harboring constitutively-active STAT3, Int. J. Cancer 127 (2010) 1259–1270.
[14] J. Chun, R.J. Choi, S. Khan, D.S. Lee, Y.C. Kim, Y.J. Nam, et al., Alantolactone suppresses inducible nitric oxide synthase and cyclooxygenase-2 expression by down-regulating NF-κB, MAPK and AP-1 via the MyD88 signaling pathway in LPS-activated RAW 264.7 cells, Int. Immunopharmacol. 14 (2012) 375–383.
[15] X.G. Mi, Z.B. Song, P. Wu, Y.W. Zhang, L.G. Sun, Y.L. Bao, et al., Alantolactone induces cell apoptosis partially through down-regulation of testes-specific protease 50 expression, Toxicol. Lett. 224 (2014) 349–355.
[16] J. Chun, E.J. Joo, M. Kang, Y.S. Kim, Platycodin D induces anoikis and caspase-mediated apoptosis via p38 MAPK in AGS human gastric cancer cells, J. Cell. Biochem. 114 (2013) 456–470.
[17] J. Chun, Y.S. Kim, Platycodin D inhibits migration, invasion, and growth of MDA-MB-231 human breast cancer cells via suppression of EGFR-mediated Akt and MAPK pathways, Chem. Biol. Interact. 205 (2013) 212–221.
[18] M.K. Pandey, B. Sung, B.B. Aggarwal, Betulinic acid suppresses STAT3 activation pathway through induction of protein tyrosine phosphatase SHP-1 in human multiple myeloma cells, Int. J. Cancer 127 (2010) 282–292.
[19] A.K. Lakkaraju, F.G. van der Goot, Calnexin controls the STAT3-mediated transcriptional response to EGF, Mol. Cell 51 (2013) 386–396.
[20] B.H. Kim, C. Won, Y.H. Lee, J.S. Choi, K.H. Noh, S. Han, et al., Sophoraflavanone G induces apoptosis of human cancer cells by targeting upstream signals of STATs, Biochem. Pharmacol. 86 (2013) 950–959.
[21] R.R. Nair, J.H. Tolentino, L.A. Hazlehurst, Role of STAT3 in transformation and drug resistance in CML, Front. Oncol. 2 (2012) 30.
[22] M.B. Gariboldi, R. Ravizza, R. Molteni, D. Osella, E. Gabano, E. Monti, Inhibition of Stat3 increases doxorubicin sensitivity in a human metastatic breast cancer cell line, Cancer Lett. 258 (2007) 181–188.
[23] X. Wang, P.J. Crowe, D. Goldstein, J.L. Yang, STAT3 inhibition, a novel approach to enhancing targeted therapy in human cancers (review), Int. J. Oncol. 41 (2012) 1181–1191.
[24] I. Souissi, I. Najjar, L. Ah-Koon, P.O. Schischmanoff, D. Lesage, S. Le Coquil, et al., A STAT3-decoy oligonucleotide induces cell death in a human colorectal carcinoma cell line by blocking nuclear transfer of STAT3 and STAT3-bound NF-κB, BMC Cell Biol. 12 (2011) 14.
[25] K.M. Quesnelle, A.L. Boehm, J.R. Grandis, STAT-mediated EGFR signaling in cancer, J. Cell. Biochem. 102 (2007) 311–319.
[26] X. Zhang, P. Yue, B.D. Page, T. Li, W. Zhao, A.T. Namanja, et al., Orally bioavailable small-molecule inhibitor of transcription factor Stat3 regresses human breast and lung cancer xenografts, Proc. Natl. Acad. Sci. U.S.A. 109 (2012) 9623–9628.
[27] M. Caraglia, G. Vitale, M. Marra, A. Budillon, P. Tagliaferri, A. Abbruzzese, Alpha-interferon and its effects on signalling pathways within cells, Curr. Protein Pept. Sci. 5 (2004) 475–485.
[28] B.B. Aggarwal, A.B. Kunnumakkara, K.B. Harikumar, S.R. Gupta, S.T. Tharakan, C. Koca, et al., Signal transducer and activator of transcription-3, inflammation, and cancer: how intimate is the relationship?, Ann. N. Y. Acad. Sci. 1171 (2009) 59–76.
[29] D.N. Burshtyn, W. Yang, T. Yi, E.O. Long, A novel phosphotyrosine motif with a critical amino acid at position -2 for the SH2 domain-mediated activation of the tyrosine phosphatase SHP-1, J. Biol. Chem. 272 (1997) 13066–13072.
[30] N. Diaz, S. Minton, C. Cox, T. Bowman, T. Gritsko, R. Garcia, et al., Activation of stat3 in primary tumors from high-risk breast cancer patients is associated with elevated levels of activated SRC and survivin expression, Clin. Cancer Res. 12 (2006) 20–28.
[31] B. Barre, A. Vigneron, N. Perkins, I.B. Roninson, E. Gamelin, O. Coqueret, The STAT3 oncogene as a predictive marker of drug resistance, Trends Mol. Med. 13 (2007) 4–11.
[32] H. Lee, A. Herrmann, J.H. Deng, M. Kujawski, G. Niu, Z. Li, et al., Persistently activated Stat3 maintains constitutive NF-κB activity in tumors, Cancer Cell 15 (2009) 283–293.
[33] A. Saha, J. Blando, E. Silver, L. Beltran, J. Sessler, J. DiGiovanni, 6-Shogaol from dried ginger inhibits growth of prostate cancer cells both in vitro and in vivo through inhibition of STAT3 and NF-κB signaling, Cancer Prev. Res. (Phila.) 7 (2014) 627–638.
[34] G.G. Mackenzie, N. Queisser, M.L. Wolfson, C.G. Fraga, A.M. Adamo, P.I. Oteiza, Curcumin induces cell-arrest and apoptosis in association with the inhibition of constitutively active NF-κB and STAT3 pathways in Hodgkin's lymphoma cells, Int. J. Cancer 123 (2008) 56–65.
[35] G. Sethi, S. Chatterjee, P. Rajendran, F. Li, M.K. Shanmugam, K.F. Wong, et al., Inhibition of STAT3 dimerization and acetylation by garcinol suppresses the growth of human hepatocellular carcinoma *in vitro* and *in vivo*, Mol. Cancer 13 (2014) 66.